Human *prx1* Gene Is a Target of Nrf2 and Is Up-regulated by Hypoxia/Reoxygenation: Implication to Tumor Biology

Yun-Jeong Kim,[1] Ji-Yeon Ahn,[1] Ping Liang,[2] Clement Ip,[3] Yuesheng Zhang,[3] and Young-Mee Park[1]

Departments of [1]Cell Stress Biology, [2]Cancer Genetics, and [3]Cancer Chemoprevention, Roswell Park Cancer Institute, Buffalo, New York

Abstract

Peroxiredoxin 1 (Prx1) has been found to be elevated in several human cancers. The cell survival–enhancing function of Prx1 is traditionally attributed to its reactive oxygen species–removing capacity, although the growth-promoting role of Prx1 independent of this antioxidant activity is increasingly gaining attention. Although much progress has been made in understanding the behavior of Prx1, little information is available on the mechanism responsible for the abnormal elevation of Prx1 level in cancer. We hypothesized that the hypoxic and unstable oxygenation microenvironment of a tumor might be crucial for *prx1* up-regulation. In this study, we cloned the human *prx1* promoter and identified nuclear factor (erythroid-derived 2)–related factor 2 (Nrf2) as a key transcription factor. Hypoxia/reoxygenation, an *in vitro* condition suited to mimic changes of oxygenation, increased Nrf2 nuclear localization and its binding to the electrophile-responsive elements located at the proximal (−536 to −528) and distal (−1429 to −1421) regions of the *prx1* promoter. A significant reduction of both steady-state and hypoxia/reoxygenation–mediated *prx1* gene expression was shown in Nrf2 knock-out cells. Our results indicated that decreased Kelch-like ECH-associated protein, Keap1, might be an important mechanism for the increased nuclear translocation and activation of Nrf2 in response to hypoxia/reoxygenation. A constitutive elevation of *prx1* mRNA and protein was observed in Keap1 knock-out cells. The above information suggests that the Nrf2-Prx1 axis may be a fruitful target for intervention with respect to inhibiting the malignant progression and/or reducing the treatment resistance of cancer cells. [Cancer Res 2007;67(2):546–54]

Introduction

Peroxiredoxins (Prx) are thiol-specific antioxidant proteins. They are found in mammals, yeast, and bacteria and are classified largely on the basis of having either one (1-Cys) or two (2-Cys) conserved cysteine residues (1). Prx1 is a major 2-Cys Prx family member. It contains a cysteine at the catalytic site (Cys^{52}) and detoxifies peroxides at the expense of Cys^{52} oxidation through intermolecular disulfide formation with the other conserved Cys^{173} residue. The disulfide bond is reduced back to the active thiol form, Cys-SH, by various mechanisms (1, 2).

Despite the initial biochemical characterization of Prx1 as a peroxide-detoxifying enzyme, the physiologic significance of its peroxidase activity is unclear because Prx1 is highly susceptible to inactivation by oxidative stress. Overoxidation of the Cys-SH to Cys-sulfinic ($-SO_2H$) or Cys-sulfonic acid ($-SO_3H$) has been reported with various Prx family members during peroxide detoxification (3). When the catalytic Cys^{52}-SH of Prx1 is overoxidized, the peroxidase activity is lost. Recent studies have suggested that overoxidation of the active site Cys in itself may be physiologically significant because it allows a mechanism of structural and functional switching of the 2-Cys Prx from a peroxidase enzyme to a molecular chaperone under stress conditions (4, 5). The wide range of effects attributed to Prx1 (6–9) may in part be explained by the physical interaction of Prx1 with growth regulatory proteins to modulate their activities (10–12).

Elevated expression of Prx1 has been observed in several human cancers (13–15), including lung cancer (16–18). We recently reported that Prx1 suppresses radiation-induced c-*Jun*-NH_2-kinase (JNK) signaling and apoptosis in lung cancer cells (19). The peroxidase activity of Prx1, however, is not essential for inhibiting JNK activation. The latter effect is mediated through the association of Prx1 with the GSTpi-JNK complex, thereby preventing JNK release from the complex. The JNK inhibitory and antiapoptotic activities of Prx1 suggest that lung cancer with high Prx1 levels is likely to be resistant not only to radiation but also to multiple anticancer agents targeting JNK and the associated apoptotic pathways. Studies by Chen et al. (20) have recently shown the role of Prx1 in radioresistance using human lung cancer xenograft models. They observed a significant growth inhibition and radiosensitization, as well as reduced metastasis of lung cancer cells stably transfected with antisense Prx1. These studies suggest that Prx1, in addition to serving as a potential prognostic marker, may also serve as a therapeutic target and/or a target for inhibiting malignant tumor progression. Delineating the molecular basis of *prx1* gene regulation is expected to provide valuable clues for the development of new intervention strategies. Although much effort has been devoted to the investigation of the various functions of Prx1, virtually nothing is known about the molecular basis of abnormal *prx1* gene regulation in cancer cells.

Hypoxia is one of the key factors influencing tumor growth and progression (21, 22). Generally speaking, hypoxia is considered a global phenomenon and is defined as an overall reduction in oxygen availability or partial pressure below critical levels (23). Tissue oxygenation within a tumor, however, is highly unstable and heterogeneous as a consequence of the architectural and functional abnormalities of the vascular network (24). Blood flow fluctuations in the tumor microvasculature can lead to perfusion-limited hypoxia in the tumor parenchyma (25, 26). In terms of the ultrastructure, tumor vasculature has numerous “holes” or “openings”, widened interendothelial junctions, and a discontinuous or absent basement membrane (27, 28). Aberrant blood vessels can be shut down locally at any time; the same defects can cause a reversal of blood flow. In addition to the reopening of the temporarily closed or blocked vessels, dynamic changes of hypoxia/reoxygenation may also occur as a result of regional angiogenesis.

Requests for reprints: Young-Mee Park, Department of Cell Stress Biology, Roswell Park Cancer Institute, Buffalo, NY 14263. Phone: 716-845-3190; Fax: 716-845-8899; E-mail: young-mee.park@roswellpark.org.

doi:10.1158/0008-5472.CAN-06-2401

We hypothesized that the hypoxic and unstable oxygenation milieu of a tumor may trigger the transactivation of the *prx1* gene via redox-sensitive transcription factors and signaling molecules. In this study, we cloned the human *prx1* upstream region and identified the critical regulatory component of *prx1* gene expression. To mimic the dynamic changes of oxygenation, we treated A549 lung cancer cells to transient hypoxia followed by reoxygenation. We showed that *prx1* is a target gene of nuclear factor (erythroid-derived 2) (NF-E2)–related factor 2 (Nrf2) and is up-regulated by hypoxia/reoxygenation. We showed a specific binding of Nrf2 to the electrophile-responsive element (EpRE) or antioxidant-responsive element located at the proximal (−536 to −528) and distal (−1429 to −1421) regions of the *prx1* promoter. We found that both steady-state *prx1* and hypoxia/reoxygenation–induced *prx1* expression are severely compromised in mouse embryonic fibroblast (MEF) cells lacking Nrf2. Lastly, our results suggest that decreased Kelch-like ECH-associated protein (Keap1) might be an important mechanism for the increased nuclear translocation and activation of Nrf2 in response to hypoxia/reoxygenation.

Materials and Methods

Cell culture. Human lung cancer A549 [American Type Culture Collection (ATCC), Manassas, VA] and 1170i (29) cells were maintained in RPMI 1640 supplemented with 10% (v/v) bovine calf serum, 100 units/mL penicillin, and 100 μg/mL streptomycin. Human prostate cancer LNCaP (ATCC) cells were grown in RPMI 1640 supplemented with 10% (v/v) fetal bovine serum containing 2 mmol/L glutamine, 100 units/mL penicillin, and 100 μg/mL streptomycin. Wi-26 (ATCC) human embryonic epithelial cells, wild-type and Nrf2 knock-out MEF (30), and Keap1 knock-out MEF (30) cells were maintained in DMEM with 10% (v/v) fetal bovine serum, 100 units/mL penicillin, and 100 μg/mL streptomycin. All cells were grown at 37°C in an atmosphere of 5% CO_2 and 95% air.

Hypoxia treatment. Hypoxia treatment was done as reported previously (31). Briefly, the culture medium was replaced with deoxygenated RPMI 1640 before hypoxia treatment at 37°C in a hypoxic chamber (Forma Scientific, Marietta, OH). Deoxygenated medium was prepared before each experiment by equilibrating the medium with a hypoxic gas mixture containing 5% CO_2, 85% N_2, and 10% H_2 at 37°C. The oxygen concentration in the hypoxic chamber and the exposure medium was maintained at <0.05% and monitored by using an oxygen indicator (Forma Scientific). All experiments were done at 70–80% confluency, and the medium pH was maintained between 7.2 and 7.4 for the duration of hypoxia exposure.

Plasmid construction. A 2,100-bp fragment of the human *prx1* promoter was isolated via PCR using the 5′-atatgctagcCAGCCTCCCAAAGTGCTGGG-3′ and 5′-atatctcgagCGGAACGGACGGGGGTGCCG-3′ primer pairs and high-fidelity platinum Taq DNA polymerase with proofreading capability (Invitrogen, Carlsbad, CA). A *Xho*I site was added to the 3′-primer, and a *Nhe*I site was added to the 5′-*prx1* primer. The PCR product was digested with *Nhe*I/*Xho*I, gel-isolated, and subcloned into the pGL3-Basic (Promega, Madison, WI) upstream of the luciferase reporter, and the construct was designated as pGL3-p2100 (−2,100/+1; +1 meaning the transcription initiation site). A series of deletion constructs were generated using pGL3-p2100 as a template. The information from various promoter analysis programs, including TransFac,[4] was taken into consideration when generating the deletion constructs. The sequences of the PCR primers were p1500 forward, 5′-atatgctagcGTTGCCAGGCTGGAGTGCAG-3′; p1000 forward, 5′-atatgctagcCCTCGTCTCTACTAAAAATA-3′; p700 forward, 5′-atatgctagcGCAAATAATTAATTATGATT-3′; p500 forward, 5′-atatgctagcTAAGTTTAGGAGTCCTGATA-3′; p300 forward, 5′-atatgctagcGCAGCTAAGACGCTTACTCC-3′; and p100 forward, 5′-atatgctagcACGAGGGAAAGCGCCGAGTC-3′. The same reverse primer, 5′-atatctcgagCGGAACGGACGGGGGTGCCG-3′, was used to generate the deletion constructs. The sequence accuracy of all constructs was confirmed by using an ABI 3700 capillary sequencer (Applied Biosystems, Foster City, CA).

Site-directed mutagenesis. Site-directed mutagenesis was done by using the GeneTailor Site-Directed Mutagenesis kit (Invitrogen). To generate mtEpRE1 (TGAATCAGC → GTAATCATA) and mtEpRE2 (TGCCTCAGC → GTCCTCATA), mtEpRE1, mt1F 5′-GGAGAGGATGGTCGTGTAACGTAATCATACTCCCAAGAT-3′ and mt1R 5′-GTTACACGACCATCCTCTCCCCGGATGAAT-3′, mtEpRE2, mt2F 5′-CCGGGTTCAAGCGATTCCCCGTCCTCATACTCCCAAGTA-3′, and mt2R 5′-GGGGAATCGCTTGAACCCGGAGGCAGAGGT-3′ were used, respectively. For the construction of the double mutant, mt1mt2, mtEpRE1 was used as a template, and site-directed mutagenesis was done using the mtEpRE2 primer pairs. The constructs were verified by DNA sequencing in both directions.

RNA isolation and reverse transcription-PCR analysis. Total cellular RNA was extracted with TRIzol Reagent (Invitrogen) according to the manufacturer's instructions. RNA concentration was determined by measuring UV absorption, and samples with comparable A_{260}/A_{280} ratios were used for reverse transcription-PCR analysis. The sequences of the PCR primer pairs used for the amplification of human *prx1, keap1*, and *β-actin* were forward 5′-ATGTCTTCAGGAAATGCTAAAAT-3′ and reverse 5′-TCACTTCTGCTTGGAGAAATATTC-3′; forward 5′-CCTGTCCCACTGCCAACTGGTGAC-3′ and reverse 5′-CCTTGCAGCGGGAGTCGGACTGCA-3′; and forward 5′-CAAGAGATGGCCACGGCTGCT-3′ and reverse 5′-TCCTTCTGCATCCTGTCGGCA-3′, respectively. The sequences of the PCR primer pairs used for the amplification of mouse *prx1* and *β-actin* were forward 5′-GTCCCACGGAGATCATTGCTTTC-3′ and reverse 5′-CCCCTGAAAGAGATACCTTCATC-3′; and forward 5′-ACTTGCGCTCAGGAGGAGCAATG-3′ and reverse 5′-GAGATGGCCACTGCCGCATCCTCTT-3′, respectively. PCR was carried out with a thermal cycler (Perkin-Elmer 9600, Boston, MA). Amplification conditions were 25 cycles for *prx1* and *β-actin*, or 30 cycles for *keap1*, of 30 s at 94°C, 30 s at 55°C, and 40 s at 72°C. The amplified products were separated by electrophoresis on a 1.5% agarose gel, stained with ethidium bromide, and photographed under UV illumination.

Transfection and reporter gene assay. Transient reporter gene assays were done by standard transfection methods using 1.5×10^4 cells in 24-well plates. Plasmid constructs (0.2 μg of reporter gene plasmid and 0.02 μg of pRLTK normalizing vector) were transfected into cells by using Fugene 6 reagent (Roche, Branchburg, NJ) according to manufacturer's instruction. Twenty-four hours after transfection, cells were exposed to hypoxia or treated with 20 μmol/L *tert*-butylhydroquinone (tBHQ), and luciferase activities were measured by the luciferase assay system (Promega). Relative luciferase activities were calculated by normalizing the *Renilla* luciferase activity from the pRLTK plasmid. All transfection experiments were done in triplicate and repeated at least thrice.

Nuclear extracts and electrophoretic mobility shift assay. Nuclear lysates were prepared as described previously (31). Briefly, cells were harvested, washed thrice with PBS, resuspended in a hypotonic buffer [10 mmol/L HEPES-KOH (pH 7.9), 1.5 mmol/L $MgCl_2$, 10 mmol/L KCl, and 0.1% NP40], and incubated on ice for 10 min. Nuclei were precipitated with 12,000 × *g* centrifugation for 10 min at 4°C. After washing once with the hypotonic buffer, nuclei were lysed in a lysis buffer [50 mmol/L Tris-HCl (pH 8.0), 150 mmol/L NaCl, and 1% Triton X-100], incubated on ice for 30 min, and precleared with 20,000 × *g* centrifugation for 15 min at 4°C. For the electrophoretic mobility shift assay, 8 μg of nuclear protein extract was incubated in 20 μL of a solution with 10 mmol/L HEPES (pH 7.9), 80 mmol/L NaCl, 10% glycerol, 1 mmol/L dithiothreitol, 1 mmol/L EDTA, 100 μg/mL poly(deoxyinosinic-deoxycytidylic acid), and radiolabeled double-stranded oligonucleotide containing the EpRE elements present in the human *prx1* promoter. EpRE-binding complexes were resolved on native 4.5% polyacrylamide gels in 0.25× Tris-borate-EDTA at 140 V for 1 h. Competition experiments were done by adding 100-fold excess of unlabeled oligonucleotides or nonspecific heat shock element (HSE) containing oligonucleotides. For Nrf2 supershift experiments, nuclear protein extract was incubated with the Nrf2 antibody (Santa Cruz Biotechnology, Santa Cruz, CA). Rabbit immunoglobulin G (Santa Cruz Biotechnology) was used as the negative control.

[4] http://transfac.gbf.de/cgi-bin/matsearch.

Chromatin immunoprecipitation assay. Chromatin immunoprecipitation assays were carried out following the previously described procedure with minor modifications (31). Briefly, formaldehyde was added directly to cells before or after hypoxia/reoxygenation. The crosslinking process was limited to <30 min because longer incubation with formaldehyde caused cells to aggregate and prevented the efficient sonication of the chromatin. After crosslinking, cells were lysed in buffer containing protease inhibitors. Nuclei were isolated, and chromatin was sheared to an average length of 250 to 500 bp using sonication. The sheared chromatin was precleared with salmon sperm DNA/protein A-sepharose and precipitated with an antibody specific to Nrf2 (2 μg/mL; Santa Cruz Biotechnology). Rabbit immunoglobulin G was used as a control to monitor nonspecific interactions. Immune complexes were adsorbed onto salmon sperm DNA/protein A-sepharose beads. After an extensive wash to reduce background, Ab/Nrf2/DNA complexes were eluted. After precipitation, DNA was resuspended in water, and PCR was carried out to amplify the EpRE1- or EpRE2-containing regions in the *prx1* promoter gene. The following primer sequences were used to amplify the two EpRE regions: EpRE1, forward 5′-GAGAGGATGGTCGTGTAACTG-3′, reverse 5′-CAGGGTTGCTGCTTTCTGTTG-3′; and EpRE2, forward 5′-TTGAGACGGAGTCTTGCTCTG-3′, reverse 5′-GTAGTCCTAGCTACTTGGGAG-3′, respectively. The intervening region between the EpRE1 and EpRE2 regions of the human *prx1* promoter was amplified as a negative control by using a forward 5′-GGATCACCTGAGGTCAGGCGT-3′ and reverse 5′-CACGCACCACCACGCCCAGCT-3′ primer pair. Triplicate PCR reactions were conducted for each sample, and the experiments were repeated at least thrice.

Western blot analysis. Cells were rinsed thrice with ice-cold PBS and lysed in radioimmunoprecipitation assay buffer [50 mmol/L Tris-Cl (pH 7.4), 1% NP40, 150 mmol/L NaCl, 1 mmol/L EDTA, 1 mmol/L phenylmethylsulfonyl fluoride, 1 μg/mL each of aprotinin and leupeptin, and 1 mmol/L Na_3VO_4]. After centrifugation at 12,000 × *g* for 30 min, the supernatant was collected, and protein concentration was determined by the Lowry method (32). Equal amounts of protein were separated on 12% (for Prx1 and Keap1) or 7.5% (for Nrf2) SDS-PAGE gel and blotted onto nitrocellulose membranes. The blots were incubated with anti-Prx1 (Lab Frontier, Seoul, Korea), anti-Nrf2 (Santa Cruz Biotechnology) or anti-Keap1 (Santa Cruz Biotechnology) antibody. Antibody to β-actin (Sigma, St. Louis, MO) or Lamin B (Santa Cruz Biotechnology) was used as a loading control. Immunoreactive bands were detected with horseradish peroxidase-conjugated secondary antibodies and enhanced chemiluminescence reagents (Amersham Biosciences, Piscataway, NJ). The experiments were repeated at least thrice.

Immunocytochemistry. Cells seeded on coverslips in six-well plates were allowed to grow for 24 h. After exposure to hypoxia or treatment with 20 μmol/L tBHQ, the cells were washed with PBS, fixed in 4% paraformaldehyde for 30 min at room temperature, permeabilized with 1% Triron X-100 for 10 min, and blocked with 1% bovine serum albumin in PBS for 15 min. The cells were then incubated with anti-Nrf2 antibody (Santa Cruz Biotechnology) for 45 min, followed by incubation with FITC-conjugated antirabbit secondary antibody (Molecular Probes, Eugene, OR) for 45 min. For filamentous actin staining, cells were incubated with rhodamine-conjugated phalloidin (Molecular Probes) for 10 min. The coverslips were mounted on slides using Vectashield mounting medium containing 4′,6-diamidino-2-phenylindole (Vector Laboratories, Burlingame, CA). Fluorescence images were visualized with the Nikon Eclipse E600 inverted microscope.

Statistical analysis. Statistical significance was examined using Student's *t* tests. The two-sample *t* test was used for two-group comparisons. Values were reported as means ± SD. *P* values <0.05 were considered significant and indicated by asterisks in the figures.

Results

Up-regulation of *prx1* expression by hypoxia/reoxygenation and multiple sequence alignment analysis of the *prx1* upstream sequences. To test whether a hypoxic and unstable oxygenation condition activates *prx1* gene expression, human lung cancer A549 cells were exposed to 4 h of hypoxia, followed by reoxygenation in a CO_2 incubator. Reverse transcription-PCR analysis showed a significant up-regulation of *prx1* expression during reoxygenation (Fig. 1*A*). The accumulation of Prx1 protein closely correlated with the mRNA level (Fig. 1*B*). Hypoxia treatment alone, however, did not up-regulate *prx1* gene expression even when the cells were treated with longer periods of hypoxia (Fig. 1*C*). The effect of an unstable oxygenation condition on *prx1* up-regulation was not unique to A549 cells. Similar responses were observed in several other cancer cell models, including human lung cancer 1170i and prostate cancer LNCaP cells (data not shown). Increased *prx1* mRNA level was reproducibly observed in reoxygenated cells regardless of the prior duration of hypoxia. These results are consistent with the hypothesis that dynamic changes of oxygenation of a tumor trigger the transcriptional activation of *prx1* expression. The human *prx1* gene may not be a target of hypoxia-inducible factor-1α because hypoxia-inducible factor-1α binding to the hypoxia-responsive element is known to increase during continuous exposure to hypoxia and to decline immediately by oxygen replenishment (21).

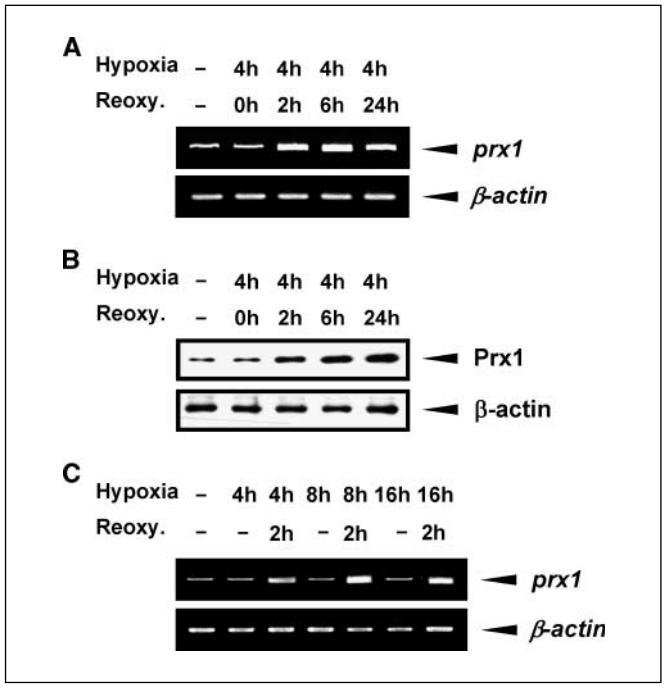

Figure 1. Up-regulation of *prx1* expression by hypoxia/reoxygenation. *A,* human lung cancer A549 cells were exposed to hypoxia for 4 h, followed by reoxygenation for 0, 2, 6, or 24 h. Total RNA was isolated, and reverse transcription-PCR analysis was carried out using primer pairs specific for human *prx1* gene. *β-actin* gene was used as a control. *B,* protein extracted from cells treated as above was subjected to Western blot analysis. Equal amounts of protein (10 μg) were separated by SDS-PAGE and probed with an antibody specific to Prx1. β-actin was used as a loading control. *C,* cells were exposed to 4, 8, or 16 h of hypoxia, followed by 2 h of reoxygenation. Total RNA was isolated, and reverse transcription-PCR was carried out using human *prx1* primer pairs. *β-actin* gene was used as a control.

Because no information is available on the transcriptional regulation of the human *prx1* gene, we carried out a computer-based sequence analysis of the mouse, rat, and human *prx1* upstream sequences. About 5 kb genomic sequences upstream of *prx1* were retrieved in Fasta format from the UCSC genome browser.[5] Multiple sequence alignment analysis was done with a

[5] http://genome.ucsc.edu.

locally installed Clustal X (33) program in combination with MEME (Multiple Em for Motif Elicitation; ref. 34), and CONREAL (CONserved Regulatory Elements anchored ALignment; ref. 35) programs. The computer-based sequence analysis revealed that the 5′ 2.1-kb segment upstream of the human *prx1* gene contains most of the sequence conservation across the three mammalian species (data not shown). No obvious hypoxia-inducible factor-1α–responsive element was found in these *prx1* upstream regions.

Cloning of the human *prx1* promoter and identification of two EpRE sites as critical cis-elements for *prx1* up-regulation in response to hypoxia. The 5′ 2.1-kb region upstream of the human *prx1* gene was PCR cloned, and the luciferase reporter vector, pGL3-2100, was generated. Genomic DNA from the Wi-26 human embryonic epithelial cells was used to avoid possible mutations of the promoter region in cancer cells. A series of deletion vectors were constructed as described in Materials and Methods for the purpose of examining the transcriptional activation of *prx1*. The pGL3-2100 reporter vector was transfected into A549 cells, and the luciferase activities were analyzed at 0, 0.5, 2, 6, or 24 h during reoxygenation after 4 h of hypoxia treatment. The luciferase activity was highest at 6 h of reoxygenation (data not shown). This time point was chosen to study the promoter activities of the deletion constructs. The importance of the 5′ −1,500 to −1,000 and −700 to −500 regions to hypoxia/reoxygenation–mediated *prx1* activation became evident from the analysis. As shown in Fig. 2*A*, a significant reduction of the promoter activity was observed in cells transfected with pGL3-1000 and pGL3-500 when compared with the pGL3-2100 transfected cells.

An examination of these two regions with the use of various promoter analysis programs, including TransFac, indicated that both regions contain potential EpRE, also known as antioxidant-responsive element. The consensus sequence of EpRE, 5′-TGAC*NNN*GC-3′, is a DNA-binding element of the transcription factor, NF-E2–related factor 2, or Nrf2 (36). The proximal EpRE site is at −536 to −528 (EpRE1), and the distal site is at −1,429 to −1,421 (EpRE2; Fig. 2*B*). The conventional EpRE displays sequence similarity to the activator protein 1 response element (5′-TGAC/GTCA-3′). One of the critical features of EpRE is the "GC" at the 3′ end of the EpRE core; this feature is met by *prx1*-EpRE1 and *prx1*-EpRE2. Suffice it to note that EpRE1 and EpRE2 possess one sequence mismatch in the fourth and third nucleotide, respectively. Previous studies have also reported a correlation between *prx1* mRNA accumulation and activation of Nrf2 (37).

To verify the significance of EpRE1 and EpRE2, EpRE1 mutant (pGL3-mtEpRE1), EpRE2 mutant (pGL3-mtEpRE2), and the double mutant (pGL3-mt1mt2) reporter vectors were constructed from pGL3-p2100 (Fig. 2*C*). The mutations were designed to disrupt the Nrf2 recognition sequences of EpRE1 and EpRE2. When pGL3-mtEpRE1 was transfected, both steady-state and hypoxia/reoxygenation–responsive reporter activities were completely lost. When pGL3-mtEpRE2 was transfected, hypoxia/reoxygenation–responsive promoter activity was significantly reduced, although EpRE1 was intact, indicating that both EpRE1 and EpRE2 are required for hypoxia/reoxygenation–mediated activation of *prx1*. The fact that the steady-state promoter activity of pGL3-mtEpRE2 was comparable to that of pGL3-2100 suggests that EpRE1, but not EpRE2, may be critical for baseline *prx1* expression.

EpRE-binding activity of Nrf2 is increased by hypoxia/reoxygenation. The EpRE-binding activities were examined during reoxygenation after 4 h of hypoxia treatment in A549 cells. As shown in Fig. 3*A*, increases of EpRE1- and EpRE2-binding activities were observed as early as 0.5 h during reoxygenation upon withdrawal from hypoxia. The EpRE-binding activities were specific because the DNA-binding complexes became undetectable when molar excess of the unlabeled competitor of the EpRE1- or EpRE2-containing probe was added. The addition of HSE, a classic stress-response element, did not inhibit EpRE-binding activities. The binding activity of EpRE1 declined with time, in contrast to the sustained activity of EpRE2. The reason for this difference is unclear, although a possible role of the adjacent sequences of the EpRE1- and EpRE2-containing probes and the profile of Nrf2 interaction with other nuclear factors may be responsible. When nuclear extracts of A549 cells were incubated with the Nrf2 antibody, the disappearance of the EpRE-binding complexes was clearly evident (Fig. 3*B*). To investigate the recruitment of Nrf2 to the EpRE sites of the human *prx1* promoter in the natural chromatin milieu, we did chromatin immunoprecipitation assays on EpRE1 and EpRE2 with the Nrf2-specific antibody. To control for possible nonspecific interactions and DNA contaminations, samples precipitated with rabbit immunoglobulin G were included. As shown in Fig. 3*C*, our results validated an increased occupancy of Nrf2 in the EpRE1 and EpRE2 regions of the *prx1* promoter in response to hypoxia/reoxygenation. The recruitment of Nrf2 to these EpRE sites was specific because no signal was detected in the immunoglobulin G control samples. We did not find an increase of Nrf2 recruitment to the nonspecific intervening region located between EpRE1 and EpRE2. The results obtained from DNA that was PCR amplified from chromatin extracts before immunoprecipitation (input) are shown for comparison.

Increased nuclear localization and transactivation of Nrf2 by hypoxia/reoxygenation. To test whether the *prx1* promoter is functional with other Nrf2 inducers, pGL3-2100 promoter activities were examined in A549 cells treated with tBHQ. The latter is one of the classic activators of Nrf2. As shown in Fig. 4*A*, treatment with 20 μmol/L tBHQ also increased the *prx1* promoter activity. Immunofluorescence studies confirmed the increased nuclear localization of Nrf2 in cells subjected to hypoxia/reoxygenation or treated with tBHQ (Fig. 4*B*). Nrf2 localization was examined by incubation with an anti-Nrf2 antibody; the location and integrity of the nucleus was probed by 4′,6-diamidino-2-phenylindole staining of the same cells. Overlaying the Nrf2 and 4′,6-diamidino-2-phenylindole images (cyan color) confirms the nuclear localization of Nrf2. In control cells, low levels of Nrf2 expression were observed in the cytoplasm and the nucleus. The Nrf2/filamentous actin overlay (orange color) images display the cytoplasmic localization of Nrf2. Nuclear fractions were then prepared, and as shown in Fig. 4*C*, there was significantly increased Nrf2 accumulation in the nucleus as shown by Western blot analysis. It should be noted that the Nrf2 band seemed at ~100 kDa, although the expected MW is at 68 kDa. The occurrence of the higher molecular mass of Nrf2 in Western blot analysis has been described by others and is suggested to represent a Nrf2-actin complex (38).

An important role of Nrf2 in *prx1* transactivation was also shown in Nrf2 knock-out cells. The accumulation of *prx1* mRNA was significantly diminished in Nrf2 −/− cells when compared with Nrf2 +/+ MEF cells (Fig. 4*D*). However, neither baseline nor hypoxia/reoxygenation–responsive expression of *prx1* mRNA was completely abolished in cells lacking Nrf2. It is conceivable that in addition to Nrf2, various regulatory factors might be involved in coordinating and relaying different cellular signals to the transcriptional machinery of the *prx1* gene, as is true for other genes involved in cell growth and survival regulation.

Keap1, an Nrf2 suppressor, is reduced by hypoxia/reoxygenation. Keap1 is known to suppress the nuclear accumulation of Nrf2. Liberation of Nrf2 from Keap1 has been suggested to stabilize cytoplasmic Nrf2 and increase its nuclear translocation and transactivation (39). Our results showed that hypoxia/reoxygenation significantly reduced Keap1 protein level in A549 cells (Fig. 5*A*). A detailed time course experiment revealed that the decrease of Keap1 occurred as early as 0.5 h of reoxygenation, which was accompanied by the simultaneous increase of Nrf2 accumulation in the nuclear fractions. Keap1 down-regulation under hypoxia/reoxygenation conditions is not unique to A549 cells. Similar results were obtained in the 1170i and LNCaP cells. When A549 and 1170i cells were reoxygenated for a longer period of time, i.e., 6 or 24 h, an additional increase of Nrf2 was noted. This is likely due to the *de novo* synthesis of Nrf2. Nrf2 itself was shown to contain an EpRE-like element in its promoter (40). Reduced Keap1 protein, however, was not due to reduced mRNA. Comparable levels of *keap1* mRNA were observed in control and hypoxic cells, suggesting an increased degradation of Keap1 during reoxygenation. Consistent with this interpretation, not only a constitutive elevation of Nrf2 protein (Fig. 5*B*) but also an increased accumulation of *prx1* mRNA and protein (Fig. 5*C*) was found in Keap1 −/− MEF cells.

Discussion

Although hypoxia is generally accepted as an important microenvironmental factor in influencing tumor progression and treatment response, it is usually regarded as a static global phenomenon. Consequently, much less attention is given to the

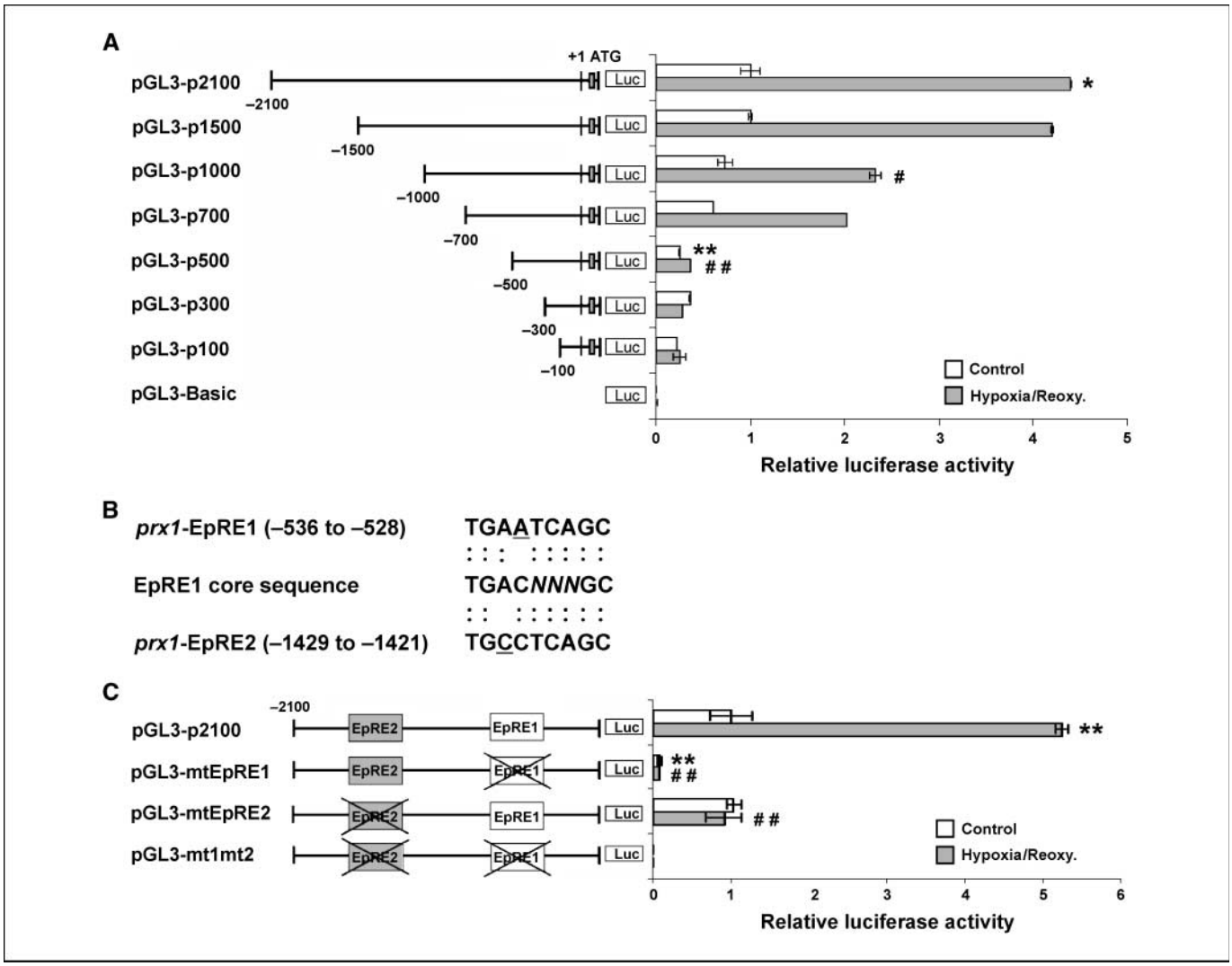

Figure 2. Analysis of hypoxia/reoxygenation–responsive *prx1* promoter activities. *A,* A549 cells were transfected with a series of *prx1* promoter reporter vectors. The pRLTK vector containing the *Renilla* luciferase gene was cotransfected to normalize the transfection efficiency. Twenty-four hours after transfection, cells were exposed to hypoxia for 4 h, followed by reoxygenation for 6 h. The data are presented as the ratio of the normalized luciferase activities. The numbers on the promoter vectors represent the positions starting from the transcription initiation site of the human *prx1* gene (+1). *, $P < 0.05$; **, $P < 0.01$, compared with control pGL3-2100 value. #, $P < 0.05$; ##, $P < 0.01$, compared with pGL3-2100 reporter activity after hypoxia/reoxygenation. *B,* EpRE1 and EpRE2 sequences present in the human *prx1* promoter were compared with the conventional EpRE core sequences. The nucleotide sequence of EpRE1 or EpRE2 that differs from the core sequence is underlined. *C,* the pGL3-mtEpRE1, pGL3-mtEpRE2, and the double mutant, pGL3-mt1mt2, were transfected into A549 cells together with the pRLTK normalizing vector. Relative luciferase activities were analyzed as described in *A*. **, $P < 0.01$, compared with control pGL3-2100 value. ##, $P < 0.01$, compared with pGL3-2100 reporter activity after hypoxia/reoxygenation.

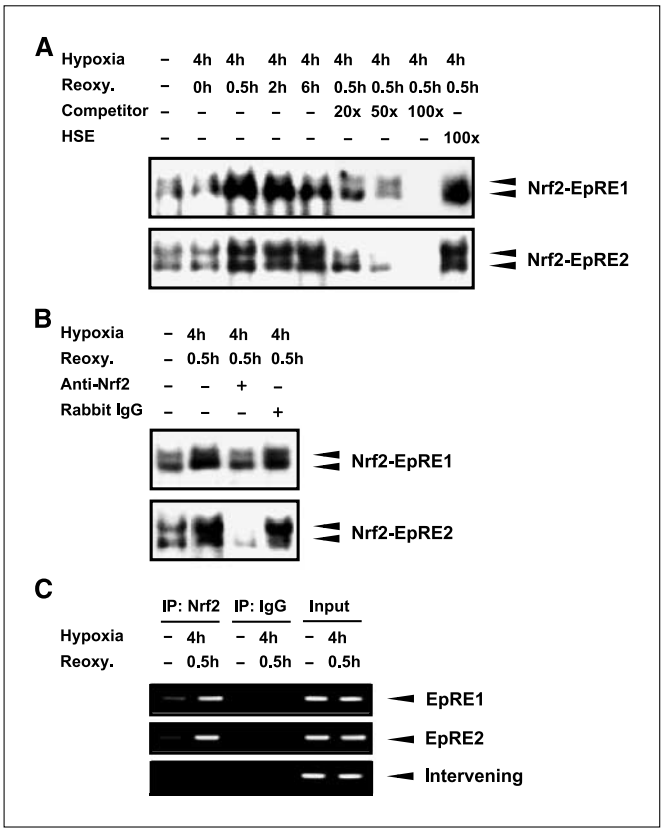

Figure 3. Binding of Nrf2 to EpRE1 and EpRE2 in response to hypoxia/reoxygenation. *A,* nuclear extracts were prepared from A549 cells immediately after 4 h of hypoxia (0 h) or 0.5, 2, or 6 h during reoxygenation. The electrophoretic mobility shift assay was done using radiolabeled EpRE1- or EpRE2-containing oligonucleotides. Unlabeled EpRE1 or EpRE2 was used as a specific competitor. Unlabeled heat shock responsive element (HSE) was used as a nonspecific competitor. Representative results from three independent experiments. *B,* nuclear extracts from cells treated with 4 h hypoxia/0.5 h reoxygenation were incubated with an anti-Nrf2 antibody. The specificity of Nrf2 binding to EpRE1 or EpRE2 was confirmed by using an antirabbit immunoglobulin G as a negative control. Representative results from three independent experiments. *C,* A549 cells treated with 4 h hypoxia/0.5 h reoxygenation were processed for ChIP assays using the primer pairs described in Materials and Methods. Input shows results obtained from DNA that was PCR amplified from chromatin extracts before immunoprecipitation. Rabbit immunoglobulin G lanes show PCR results obtained after immunoprecipitation with rabbit immunoglobulin G. Gels are representative of three independent experiments.

impact of the dynamic changes of tumor oxygenation in regulating the behavior of cancer cells. Our results showed that human *prx1* is up-regulated by hypoxia/reoxygenation, an *in vitro* condition that is suited to mimic the hypoxic and unstable oxygenation milieu of a tumor. We concluded that Nrf2 is one of the key transcription factors for *prx1* gene expression. Increased nuclear localization and transactivation of Nrf2 by hypoxia/reoxygenation was accompanied by a reduced level of Keap1 protein. Promoter cloning and characterization revealed two EpRE sites located at −536 to −528 (EpRE1) and −1,429 to −1,421 (EpRE2) as the Nrf2-binding sites responsible for both steady-state and hypoxia/reoxygenation–responsive regulation of *prx1* expression.

Based on the above information, we propose that the elevated expression of Prx1 observed in various cancers (13–18) may be explained in part by the activation of Nrf2 in response to the hypoxic and unstable oxygenation microenvironment of a tumor. The subpopulation of cells with elevated Prx1 may thus acquire an aggressive survival advantage that contributes to the malignant progression of cancer. Considering that Nrf2 is a major transcription factor responsible for the activation of EpRE-mediated drug–metabolizing/detoxifying genes (41), the impact of Nrf2 stimulation may also extend to the emergence of treatment-resistant cancers. Studies have suggested that the association of Nrf2 with Keap1 in response to electrophiles promotes Nrf2 degradation and prevents it from translocating to the nucleus (42, 43). However, a number of EpRE-dependent genes, including *prx1*, are constitutively expressed by Nrf2. This implies the existence of activated Nrf2 in the nucleus; the assumption is consistent with our immunocytochemistry results showing the nuclear expression of Nrf2 in control cells. How nuclear Nrf2 escapes Keap1 repression and activates the steady-state expression of its target genes is still an unresolved question. The precise mechanism by which Keap1 sequesters Nrf2 in the cytoplasm without causing its degradation is another question that begs for an answer. Given the short half-life of Nrf2, the purpose of its sequestration is also puzzling. An alternative role of Keap1 might be as a negative feedback regulator in returning Nrf2, and thereby the expression of Nrf2 target genes, to steady-state level after its activation (44). Such an event would have entailed the repression of Nrf2 by Keap1 only after Nrf2 exerts its transcriptional activity in the nucleus.

Phosphorylation of Nrf2 by various kinases has been implicated in its stabilization and nuclear localization and transactivation (38, 45–47). For example, phosphorylation at Ser^{40} by PKC (46) may disrupt Nrf2-Keap1 interaction and Nrf2 degradation in response to hypoxia/reoxygenation. The phosphoinositide-3-kinase pathway has also been proposed to regulate Nrf2 through actin rearrangement in response to oxidative stress (38). Various mitogen-activated protein kinases may regulate Nrf2 either positively or negatively depending on the signaling context of a particular EpRE-containing gene (45). It seems that Nrf2 transactivation is dependent on a number of regulatory mechanisms acting in concert to increase or decrease the Nrf2 protein level and to promote or suppress its stabilization and accumulation in the nucleus. However, the exact target sites of phosphorylation and the underlying mechanisms regulating Nrf2 stability and function have yet to be delineated. Additionally, the interaction of Nrf2 with other nuclear factors or components of the general transcriptional machinery may also influence Nrf2 activity (48). These may explain the variable levels of Prx1 expression observed in cancer cells and tissues.

Keap1 binds to the Neh2 domain of Nrf2 through the double glycine repeat and the COOH-terminal region to assert its repressive activity on Nrf2 (39, 49). Recent studies suggest a possible role of genetic abnormalities in Keap1 in eliminating or reducing its association with Nrf2 as a way of increasing Nrf2 activity in lung cancer cells (49, 50). Padmanabhan et al. (49) found the occurrence of glycine to cysteine mutations in the double glycine repeat domain of Keap1 in one lung cancer tissue (G430C, G/G to T/G) and in two lung cancer cell lines (G364C, G/G to TT). These mutations were found to alter the local conformation of Keap1 in the DC domain (double glycine repeat and COOH-terminal region) and to result in a reduced affinity of Keap1 to Nrf2. Because the mutations in Keap1 lead to a reduction, but not a complete abolishment, of its interaction with Nrf2, it is possible that the structural defects of Keap1 may augment the functionality of Nrf2 and give rise to a higher expression of *prx1* in response to an unstable oxygenation condition. Singh et al. (50) did a systematic analysis of the Keap1 genomic locus and sequencing of

Keap1 gene in 12 lung cancer cell lines and 54 tumor tissues. They showed that a mutation or an inactivation of Keap1 is a frequent event in lung cancer. Various mutations in Keap1 gene were found in 6 cell lines and 10 tumor tissues. Loss of heterozygosity was detected in the genomic locus of Keap1 (19q13.2) in 61% of the cell lines and 41% of the tumor samples that were examined. These findings led to a suggestion that the loss of function in Keap1 leads to a constitutive activation of Nrf2 in lung cancer.

These recent findings are consistent with our results in Keap1 −/− MEF cells in which we found not only an elevation of Nrf2 activity, but also an increased accumulation of *prx1* mRNA and protein. It is noteworthy, however, that not all cancer cell lines or tissues exhibit the genetic abnormalities in Keap1. Singh et al. (50) indeed noted an elevated Nrf2 activity in a number of tumor samples that contain a wild-type Keap1 gene, clearly suggesting that there are other mechanisms operating in these tissues. Our results offer a possible explanation that the decrease of Keap1 in an unstable oxygenation milieu of a tumor could serve as an important mechanism for the increased activation of Nrf2 in cells that contain a wild-type or a mutated but functional Keap1. The A549 cell line was found to possess a G-T transversion in the fourth exon of Keap1. This particular mutation, however, does not seem to affect the function of Keap1 in suppressing Nrf2 activation. Our results show that Keap1 suppresses an activation of Nrf2 in A549 cells as effectively as in other cell lines that were examined. Decrease of Keap1 by hypoxia/reoxygenation consistently released Nrf2 from Keap1 and enhanced a nuclear localization and activation of Nrf2 in several cell models including A549 (Figs. 4 and 5). The functional significance of various Keap1 mutations found in lung cancer cell lines and tissues warrants future investigation.

Hypoxia has been proposed to function as a microenvironmental pressure to select for a subset of cancer cells with an increased ability to survive and proliferate. The activation of Nrf2 and the up-regulation of *prx1* expression by changes of oxygenation are likely to contribute to the malignant progression of cancer and to modify the efficacy of chemo- and radiotherapies. The information provided in the current study suggests that the Nrf2-Prx1 axis may serve as a fruitful target for cancer prognosis and therapy. Identifying the key regulatory components and understanding the molecular basis of *prx1* gene regulation by Nrf2 are critical to the

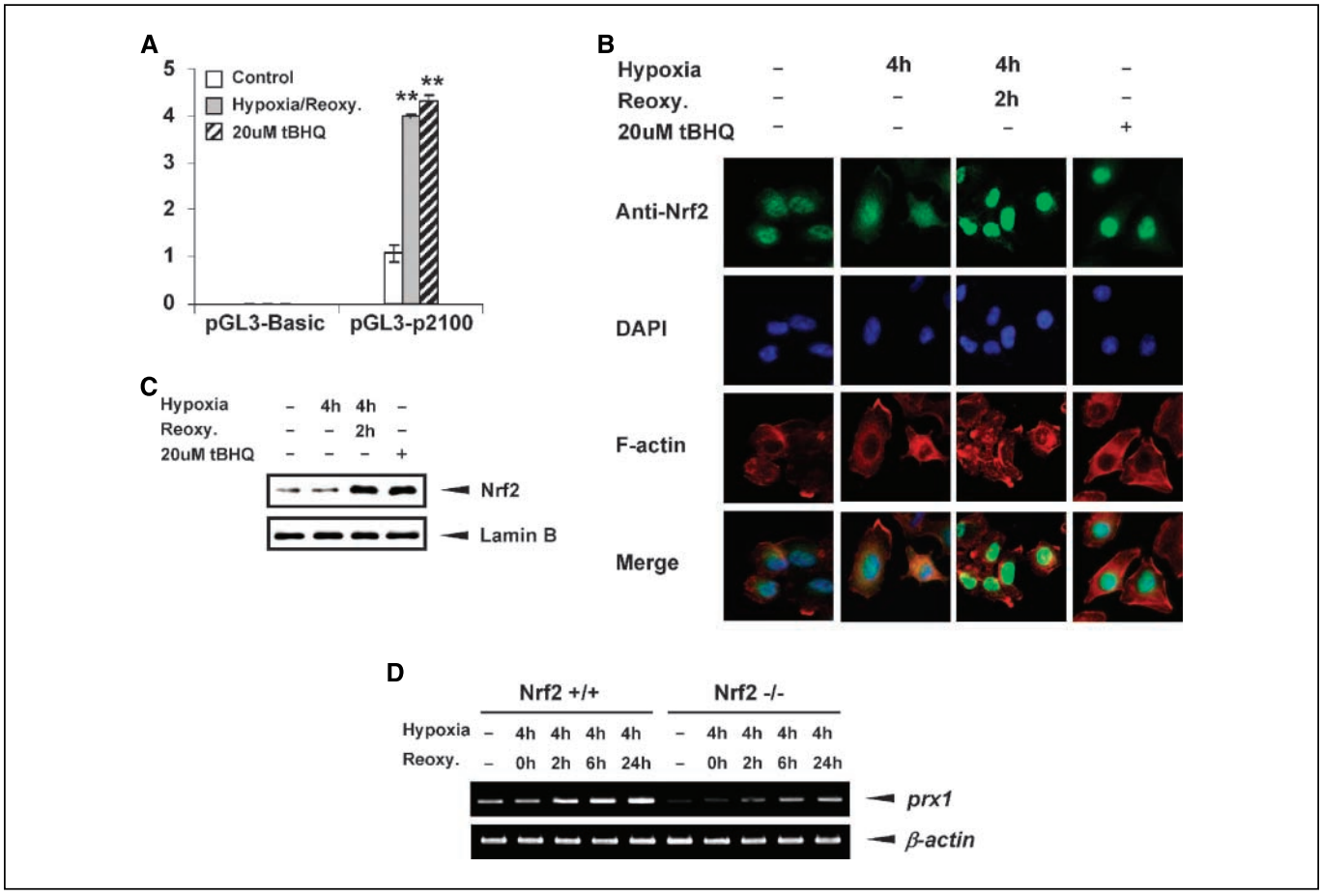

Figure 4. Stabilization of Nrf2 in the nucleus by hypoxia/reoxygenation. *A,* pGL3-p2100 was transfected into A549 cells together with pRLTK. Twenty-four hours after transfection, cells were treated with 4 h hypoxia/6 h reoxygenation or 20 μM tBHQ for 3 h. Luciferase activities were analyzed in cell extracts. **, $P < 0.01$, compared with control pGL3-2100 value. *B,* A549 cells were treated with 4 h hypoxia/2 h reoxygenation or 20 μM tBHQ for 3 h. Immunocytochemistry was done using an anti-Nrf2 antibody and FITC-conjugated secondary antibody. The location of the nuclei was visualized using 4′,6-diamidino-2-phenylindole (blue) counterstaining. Filamentous actin was stained with rhodamine-conjugated phalloidin for cytoplasmic counterstaining. The 4′,6-diamidino-2-phenylindole and filamentous actin images of the same field are shown separately or merged with the Nrf2 immunofluorescence images. *C,* equal amounts of nuclear protein (10 μg) from cells treated as described in *B* were subjected to Western blot analysis using an anti-Nrf2 antibody. Analysis of lamin B expression was done as a loading control for nuclear fraction. Representative results from three independent experiments are shown. *D,* Nrf2 +/+ and Nrf2 −/− MEF cells were exposed to 4 h of hypoxia, followed by 0, 2, 6, or 24 h of reoxygenation. Total RNA was isolated, and reverse transcription-PCR analysis was done by using primer pairs specific for the mouse *prx1* gene. *β-actin* gene was analyzed as a control. Representative results from three independent experiments are shown.

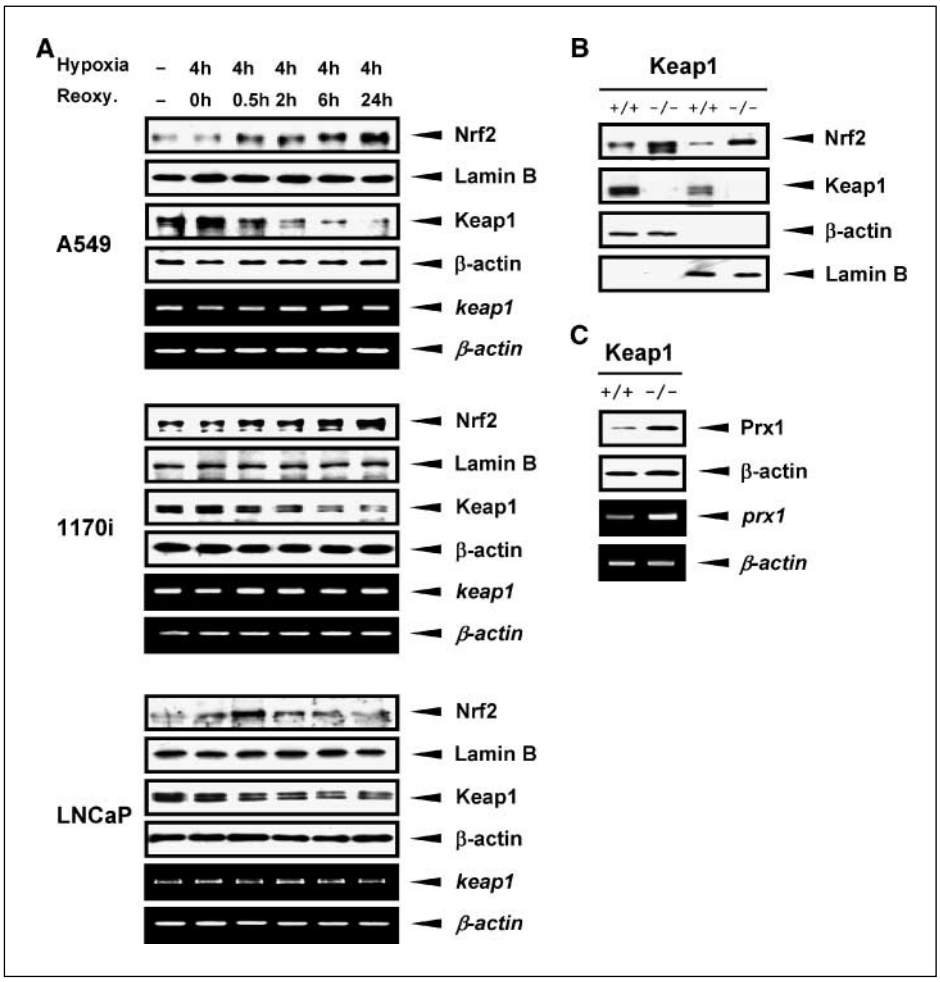

Figure 5. Reduction of Keap1 protein in response to hypoxia/reoxygenation. *A,* A549, 1170i, and LNCaP cells were exposed to 4 h of hypoxia and reoxygenated for 0, 0.5, 2, 6, or 24 h. Nuclear and cytosolic protein extracts were prepared from each cell line and subjected to Western blot analysis with an anti-Nrf2 and an anti-Keap1 antibody, respectively. Lamin B is a loading control for nuclear fraction, and β-actin is a loading control for cytosolic fraction. Total RNA was isolated from and reverse transcription-PCR was done using the primer pairs specific for the human *keap1* mRNA. *β-actin* gene was analyzed as a control. *B,* equal amounts of cytoplasmic and nuclear protein from Keap1 +/+ and Keap1 −/− MEF cells were subjected to Western blot analysis using an anti-Nrf2 or anti-Keap1 antibody. Western blots of β-actin and lamin B were carried out as the loading control for cytoplasmic and nuclear protein, respectively. *C,* total protein extract from Keap1 +/+ or −/− cells was subjected to Western blot using an antibody specific to Prx1. β-actin was used as a loading control. Total RNA from Keap1 +/+ or −/− cells were subjected to reverse transcription-PCR analysis using primer pairs specific to the mouse *prx1*. Mouse *β-actin* gene was analyzed as a control.

development of intervention strategies. Future research will be aimed at finding out whether Nrf2-Prx1 activation can be suppressed by genetic and/or pharmacologic approaches, and whether suppressing the Nrf2-Prx1 axis will inhibit the malignant progression or reverse treatment resistance in preclinical models. It would be important to investigate whether the Nrf2-Prx1 axis is dysregulated in lung cancer and other malignancies, and whether it correlates with a poor clinical outcome.

Acknowledgments

Received 6/30/2006; revised 10/31/2006; accepted 11/14/2006.

Grant support: NIH grants CA109480, CA111846, Department of Defense grant PC050127, and Cancer Center Support grant CA16056.

The costs of publication of this article were defrayed in part by the payment of page charges. This article must therefore be hereby marked *advertisement* in accordance with 18 U.S.C. Section 1734 solely to indicate this fact.

We are grateful to Dr. Masayuki Yamamoto (Center for Tsukuba Advanced Research Alliance, University of Tsukuba, Japan) for kindly providing the wild-type and knock-out Nrf2 and Keap1 MEF cells.

References

1. Rhee SG, Kang SW, Chang TS, Jeong W, Kim K. Peroxiredoxin, a novel family of peroxidases. IUBMB Life 2001;52:35–41.
2. Wood ZA, Schroder E, Robin Harris J, Poole LB. Structure, mechanism and regulation of peroxiredoxins. Trends Biochem Sci 2003;28:32–40.
3. Rabilloud T, Heller M, Gasnier F, et al. Proteomics analysis of cellular response to oxidative stress. Evidence for *in vivo* overoxidation of peroxiredoxins at their active site. J Biol Chem 2002;277:19396–401.
4. Jang HH, Lee KO, Chi YH, et al. Two enzymes in one; two yeast peroxiredoxins display oxidative stress-dependent switching from a peroxidase to a molecular chaperone function. Cell 2004;117:625–35.
5. Moon JC, Hah YS, Kim WY, et al. Oxidative stress-dependent structural and functional switching of a human 2-Cys peroxiredoxin isotype II that enhances HeLa cell resistance to H_2O_2-induced cell death. J Biol Chem 2005;280:28775–84.
6. Ishii T, Yamada M, Sato H, et al. Cloning and characterization of a 23-kDa stress-induced mouse peritoneal macrophage protein. J Biol Chem 1993;268:18633–6.
7. Kawai S, Takeshita S, Okazaki M, Kikuno R, Kudo A, Amann E. Cloning and characterization of OSF-3, a new member of the MER5 family, expressed in mouse osteoblastic cells. J Biochem (Tokyo) 1994;115:641–3.
8. Shau H, Kim A. Identification of natural killer enhancing factor as a major antioxidant in human red blood cells. Biochem Biophys Res Commun 1994;199:83–8.
9. Neumann CA, Krause DS, Carman CV, et al. Essential role for the peroxiredoxin Prdx1 in erythrocyte antioxidant defence and tumour suppression. Nature 2003;424:561–5.
10. Wen ST, Van Etten RA. The PAG gene product, a stress-induced protein with antioxidant properties, is an Abl SH3-binding protein and a physiological inhibitor of c-Abl tyrosine kinase activity. Genes Dev 1997;11:2456–67.
11. Mu ZM, Yin XY, Prochownik EV. Pag, a putative tumor suppressor, interacts with the Myc Box II domain of c-Myc and selectively alters its biological function and target gene expression. J Biol Chem 2002;277:43175–84.
12. Jung H, Kim T, Chae HZ, Kim KT, Ha H. Regulation of macrophage migration inhibitory factor and thiol-specific antioxidant protein PAG by direct interaction. J Biol Chem 2001;276:15504–10.
13. Yanagawa T, Ishikawa T, Ishii T, et al. Peroxiredoxin I expression in human thyroid tumors. Cancer Lett 1999;145:127–32.
14. Yanagawa T, Iwasa S, Ishii T, et al. Peroxiredoxin I expression in oral cancer: a potential new tumor marker. Cancer Lett 2000;156:27–35.
15. Noh DY, Ahn SJ, Lee RA, Kim SW, Park IA, Chae HZ.

Overexpression of peroxiredoxin in human breast cancer. Anticancer Res 2001;21:2085–90.
16. Chang JW, Jeon HB, Lee JH, et al. Augmented expression of peroxiredoxin I in lung cancer. Biochem Biophys Res Commun 2001;289:507–12.
17. Lehtonen ST, Svensk AM, Soini Y, et al. Peroxiredoxins, a novel protein family in lung cancer. Int J Cancer 2004;111:514–21.
18. Chang JW, Lee SH, Jeong JY, et al. Peroxiredoxin-I is an autoimmunogenic tumor antigen in non-small cell lung cancer. FEBS Lett 2005;579:2873–7.
19. Kim YJ, Lee WS, Ip C, Chae HZ, Park EM, Park YM. Prx1 suppresses radiation-induced c-*Jun* NH_2-terminal kinase signaling in lung cancer cells through interaction with the glutathione *S*-transferase Pi/c-*Jun* NH_2-terminal kinase complex. Cancer Res 2006;66:7136–42.
20. Chen MF, Keng PC, Shau H, et al. Inhibition of lung tumor growth and augmentation of radiosensitivity by decreasing peroxiredoxin I expression. Int J Radiat Oncol Biol Phys 2006;64:581–91.
21. Harris AL. Hypoxia—a key regulatory factor in tumour growth. Nat Rev Cancer 2002;2:38–47.
22. Greco O, Marples B, Joiner MC, Scott SD. How to overcome (and exploit) tumor hypoxia for targeted gene therapy. J Cell Physiol 2003;197:312–25.
23. Zander R, Vaupel P. Proposal for using a standardized terminology on oxygen transport to tissue. Adv Exp Med Biol 1985;191:965–70.
24. Vaupel P, Kallinowski F, Okunieff P. Blood flow, oxygen and nutrient supply, and metabolic microenvironment of human tumors: a review. Cancer Res 1989; 49:6449–65.
25. Brown JM. Evidence for acutely hypoxic cells in mouse tumours, and a possible mechanism of reoxygenation. Br J Radiol 1979;52:650–6.
26. Kimura H, Braun RD, Ong ET, et al. Fluctuations in red cell flux in tumor microvessels can lead to transient hypoxia and reoxygenation in tumor parenchyma. Cancer Res 1996;56:5522–8.
27. Brown JM, Giaccia AJ. The unique physiology of solid tumors: opportunities (and problems) for cancer therapy. Cancer Res 1998;58:1408–16.
28. Dewhirst MW. Concepts of oxygen transport at the microcirculatory level. Semin Radiat Oncol 1998;8:143–50.
29. Klein-Szanto AJ, Iizasa T, Momiki S, et al. A tobacco-specific *N*-nitrosamine or cigarette smoke condensate causes neoplastic transformation of xenotransplanted human bronchial epithelial cells. Proc Natl Acad Sci U S A 1992;89:6693–7.
30. Wakabayashi N, Dinkova-Kostova AT, Holtzclaw WD, et al. Protection against electrophile and oxidant stress by induction of the phase 2 response: fate of cysteines of the Keap1 sensor modified by inducers. Proc Natl Acad Sci U S A 2004;101:2040–5.
31. Park SY, Kim YJ, Gao AC, et al. Hypoxia increases androgen receptor activity in prostate cancer cells. Cancer Res 2006;66:5121–9.
32. Lowry OH, Rosebrough NJ, Farr AL, Randall RJ. Protein measurement with the Folin phenol reagent. J Biol Chem 1951;193:265–75.
33. Jeanmougin F, Thompson JD, Gouy M, Higgins DG, Gibson TJ. Multiple sequence alignment with Clustal X. Trends Biochem Sci 1998;23:403–5.
34. Bailey TL, Elkan C. Fitting a mixture model by expectation maximization to discover motifs in biopolymers. Proc Int Conf Intell Syst Mol Biol 1994;2:28–36.
35. Berezikov E, Guryev V, Plasterk RH, Cuppen E. CONREAL: conserved regulatory elements anchored alignment algorithm for identification of transcription factor binding sites by phylogenetic footprinting. Genome Res 2004;14:170–8.
36. Nguyen T, Sherratt PJ, Pickett CB. Regulatory mechanisms controlling gene expression mediated by the antioxidant response element. Annu Rev Pharmacol Toxicol 2003;43:233–60.
37. Ishii T, Itoh K, Takahashi S, et al. Transcription factor Nrf2 coordinately regulates a group of oxidative stress-inducible genes in macrophages. J Biol Chem 2000;275: 16023–9.
38. Kang KW, Lee SJ, Park JW, Kim SG. Phosphatidylinositol 3-kinase regulates nuclear translocation of NF-E2-related factor 2 through actin rearrangement in response to oxidative stress. Mol Pharmacol 2002;62: 1001–10.
39. Itoh K, Wakabayashi N, Katoh Y, et al. Keap1 represses nuclear activation of antioxidant responsive elements by Nrf2 through binding to the amino-terminal Neh2 domain. Genes Dev 1999;13:76–86.
40. Kwak MK, Itoh K, Yamamoto M, Kensler TW. Enhanced expression of the transcription factor Nrf2 by cancer chemopreventive agents: role of antioxidant response element-like sequences in the nrf2 promoter. Mol Cell Biol 2002;22:2883–92.
41. Rushmore TH, Kong AN. Pharmacogenomics, regulation and signaling pathways of phase I and II drug metabolizing enzymes. Curr Drug Metab 2002;3:481–90.
42. Velichkova M, Hasson T. Keap1 regulates the oxidation-sensitive shuttling of Nrf2 into and out of the nucleus via a Crm1-dependent nuclear export mechanism. Mol Cell Biol 2005;25:4501–13.
43. Zhang DD, Hannink M. Distinct cysteine residues in Keap1 are required for Keap1-dependent ubiquitination of Nrf2 and for stabilization of Nrf2 by chemopreventive agents and oxidative stress. Mol Cell Biol 2003; 23:8137–51.
44. Nguyen T, Sherratt PJ, Nioi P, Yang CS, Pickett CB. Nrf2 controls constitutive and inducible expression of ARE-driven genes through a dynamic pathway involving nucleocytoplasmic shuttling by Keap1. J Biol Chem 2005; 280:32485–92.
45. Kong AN, Owuor E, Yu R, et al. Induction of xenobiotic enzymes by the MAP kinase pathway and the antioxidant or electrophile response element (ARE/EpRE). Drug Metab Rev 2001;33:255–71.
46. Huang HC, Nguyen T, Pickett CB. Phosphorylation of Nrf2 at Ser-40 by protein kinase C regulates antioxidant response element-mediated transcription. J Biol Chem 2002;277:42769–74.
47. Numazawa S, Ishikawa M, Yoshida A, Tanaka S, Yoshida T. Atypical protein kinase C mediates activation of NF-E2–related factor 2 in response to oxidative stress. Am J Physiol Cell Physiol 2003;285:C334–42.
48. Nguyen T, Yang CS, Pickett CB. The pathways and molecular mechanisms regulating Nrf2 activation in response to chemical stress. Free Radic Biol Med 2004; 37:433–41.
49. Padmanabhan B, Tong KI, Ohta T, et al. Structural basis for defects of Keap1 activity provoked by its point mutations in lung cancer. Mol Cell 2006;21:689–700.
50. Singh A, Misra V, Thimmulappa RK, et al. Dysfunctional Keap1–2 interaction in non-small-cell lung cancer. PLoS Med 2006;3:1–12.